Assessment of Two Theoretical Methods to Estimate Potentiometric Titration Curves of Peptides: Comparison with Experiment

Joanna Makowska,[†,‡] Katarzyna Bagińska,[†] Mariusz Makowski,[†,‡] Anna Jagielska,[‡] Adam Liwo,[†,‡] Franciszek Kasprzykowski,[†] Lech Chmurzyński,[†] and Harold A. Scheraga*[,‡]

Faculty of Chemistry, University of Gdańsk, Sobieskiego 18, 80-952 Gdańsk, Poland, and Baker Laboratory of Chemistry and Chemical Biology, Cornell University, Ithaca, New York 14853-1301

Received: August 25, 2005; In Final Form: January 3, 2006

We compared the ability of two theoretical methods of pH-dependent conformational calculations to reproduce experimental potentiometric titration curves of two models of peptides: Ac-K_5-NHMe in 95% methanol (MeOH)/5% water mixture and Ac-XX(A)$_7$OO-NH_2 (XAO) (where X is diaminobutyric acid, A is alanine, and O is ornithine) in water, methanol (MeOH), and dimethyl sulfoxide (DMSO), respectively. The titration curve of the former was taken from the literature, and the curve of the latter was determined in this work. The first theoretical method involves a conformational search using the electrostatically driven Monte Carlo (EDMC) method with a low-cost energy function (ECEPP/3 plus the SRFOPT surface-solvation model, assumming that all titratable groups are uncharged) and subsequent reevaluation of the free energy at a given pH with the Poisson−Boltzmann equation, considering variable protonation states. In the second procedure, molecular dynamics (MD) simulations are run with the AMBER force field and the generalized Born model of electrostatic solvation, and the protonation states are sampled during constant-pH MD runs. In all three solvents, the first pK_a of XAO is strongly downshifted compared to the value for the reference compounds (ethylamine and propylamine, respectively); the water and methanol curves have one, and the DMSO curve has two jumps characteristic of remarkable differences in the dissociation constants of acidic groups. The predicted titration curves of Ac-K_5-NHMe are in good agreement with the experimental ones; better agreement is achieved with the MD-based method. The titration curves of XAO in methanol and DMSO, calculated using the MD-based approach, trace the shape of the experimental curves, reproducing the pH jump, while those calculated with the EDMC-based approach and the titration curve in water calculated using the MD-based approach have smooth shapes characteristic of the titration of weak multifunctional acids with small differences between the dissociation constants. Nevertheless, quantitative agreement between theoretically predicted and experimental titration curves is not achieved in all three solvents even with the MD-based approach, which is manifested by a smaller pH range of the calculated titration curves with respect to the experimental curves. The poorer agreement obtained for water than for the nonaqueous solvents suggests a significant role of specific solvation in water, which cannot be accounted for by the mean-field solvation models.

1. Introduction

Calculation of the pK_a values of ionizable groups in proteins and the influence of pH on their conformation are still one of the most difficult problems in computational chemistry. The protonation state of acidic and basic sites is of great importance for biomolecular function, and much effort has therefore been devoted to understand the pH titration of biomolecules.[1−6] The protonation state of a titratable group is determined by the solvent pH and the pK_a of the group. The pK_a of a given group is in turn influenced by its electrostatic environment, which is determined by the protein conformation and protonation state of other titratable groups.

Only a few approaches exist for conformational energy calculations without assuming a fixed degree of protonation of the acidic and basic groups in the molecule. One of them was developed by our group.[7−13] We solved the Poisson−Boltzmann (PB) equation by using the multigrid boundary element (MBE) method[14−16] to compute the free energy of electrostatic solvation and to compute the Boltzmann average over all protonation states to estimate the mean degree of protonation of a given amino acid group for a given pH value. This approach will hereafter be referred to as EDMC/PB/pH. To lower the computational cost, the ionic strength is assumed to be zero in the EDMC/PB/pH approach, which means that it is the Poisson and not the Poisson−Boltzmann equation that is actually solved. The calculation of the free energy of electrostatic solvation is accurate, but the cost of calculating the solvation component is high. To avoid this problem, the conformational search is carried out by assuming a fixed ionization state of the ionizable groups and the inexpensive surface-solvation model. Therefore, the set of conformations thus found might be incomplete. The free energy of this set is then reevaluated at each pH with the Poisson−Boltzmann equation, allowing for variation of the protonation state of each ionizable residue.[9,11−13]

A number of models have been proposed for performing molecular dynamics (MD) calculations at constant pH with

* Author to whom correspondence should be addressed. Phone: (607) 255 4034. Fax: (607) 254-4700. E-mail: has5@cornell.edu.
† University of Gdańsk.
‡ Cornell University.

10.1021/jp054814j CCC: $33.50
Published on Web 02/03/2006

dynamic protonation states.[16−19] Each of these uses Monte Carlo sampling to select protonation states based on calculated free energy differences between the possible protonation states. Recently an approach to molecular dynamics simulations at constant pH, based on the generalized Born implicit solvation model (GB) has been developed.[20,21] This approach will hereafter be referred to as MD/GB/pH. This method combines the best aspects of the discrete protonation state models developed thus far[16−19] and involves much lower computational cost compared to that involved in solving the Poisson−Boltzmann equation.[14−16,22−24] As opposed to the EDMC/PB/pH method,[9,11−13] the same GB electrostatics model is applied for calculating the protonation state, transition energies, and dynamics; hence, the potential energy function used in the sampling of protonation states is consistent with that used in conformational sampling. Furthermore, sampling and calculation of transition energies using GB is fast, because there is no need for solvent equilibration, as opposed to MD simulations with explicit solvent, in which the solvent must be equilibrated after changing protonation state.[17,19]

The quality of theoretical modeling of the ionization states of titratable groups in peptides can be assessed by comparing the experimental pH titration curves with those calculated theoretically. Most of the theoretical studies of proteolytic equilibria in peptides and proteins are concerned with the shift of the pK_a of isolated groups.[25−28] The agreement with the experimental pK_a values is within 1−2 logarithmic units on average, and theory usually predicts the direction of the shift of the pK_a from that of a single amino acid residue correctly. However, a harder test for the capability of theoretical methods to reproduce the titration behavior of peptides and proteins appears when a compound possesses multiple titratable groups with comparable reference pK_a values located close to each other so that a change of the protonation state of one of them can influence the electrostatic potential and, consequently, the proton affinity of the other ones. In the case of peptides, another difficulty is the fact that these compounds exist in an equilibrium of interconverting conformations. In our recent work,[29] we compared the theoretical pH titration curves calculated with the EDMC/PB/pH approach for Ac-K_5-NHMe and Ac-K-A_{11}-KGGY-NH_2 in water and methanol with those determined potentiometrically. We found that, for Ac-K_5-NHMe, the theoretical prediction was quite consistent with the experimental curve; however, for the second peptide, agreement with experiment was obtained only after the ensemble was reduced to those conformations containing a (Tyr)−OH$\cdots{}^+H_3N$−(Lys) salt bridge.

In this work, we carried out potentiometric titrations of a model alanine-based peptide, Ac-XX$(A)_7$OO-NH_2 (XAO) (where X is diaminobutyric acid, A is alanine, and O is ornithine) in water, methanol, and dimethyl sulfoxide (DMSO), respectively. We chose this sequence because only basic groups are present, and therefore, specific features of conformation (such as salt bridges) cannot influence the degree of ionization. Therefore, the calculated titration profiles should be less sensitive to inaccuracies inherent in the force fields applied compared to those of the peptide studied in our earlier work.[29] Moreover, recent studies by Kallenbach and co-workers[30] suggested that the XAO peptide possesses a stable polyproline II structure. In view of the fact that peptide conformation can be strongly influenced by pH because the protonation state of the titratable groups changes with pH, it is desirable to determine the ionization state of XAO in the pH range applied in the structure-determination experiments.[30] Using both the EDMC/PB/pH and MD/GB/pH approaches, we computed the theoretical pH titration curves of XAO in water, methanol, and DMSO, respectively. We also calculated the theoretical titration curve of the Ac-K_5-NHMe peptide in 95% MeOH/5% H_2O by using the MD/GB/pH method and compared it with the experimental curve reported in the literature[31] and with the theoretical titration curve already estimated by us by using the EDMC/PB/pH approach.[29]

2. Methods

2.1. Experimental Methods. *2.1.1. Chemicals.* All Fmoc amino acids were purchased from Peptides International. 1-Hydroxybenzotriazole (1-HOBt), piperidine, trifluoroacetic acid (TFA), and trifluoroethanol (TFE) were purchased from Lancaster. 1,3-Diisopropylcarbodiimide (DIPCI), *N*-acetylimidazole, and potassium hydroxide were obtained from Sigma-Aldrich. Acetonitrile for high-performance liquid chromatography (HPLC) was obtained from LabScan. Methanol (HPLC grade) was purchased from Sigma-Aldrich and contained less than 0.02% of water. All compounds were used without further purification. Water was purified using the Milli-Q system (Millipore) whereas *N*,*N*-dimethylformamide (DMF; obtained from LabScan) and dimethyl sulfoxide (DMSO; obtained from Sigma Aldrich) were distilled under reduced pressure and then kept over a 0.4 nm molecular sieve.

2.1.2. Peptide Synthesis. XAO was synthesized on a 0.19 mmol scale by the solid-phase method using the Fmoc strategy, an automated 9050 Plus PepSynthesizer with the enhanced monitoring option (Millipore), and a TentaGel R RAM resin (RAPP Polymer). N^{α}-Fmoc amino acids were in a 4-fold excess over the required amount of peptide, and DIPCI was used as a coupling agent. Synthesis was carried out in the presence of 1-HOBt. The Fmoc group was removed using 20% piperidine in DMF added to the resin-bound peptide, followed by acetylation with 10 cm^3 of 1 M *N*-acetylimidazole solution in DMF for about 18 h at room temperature. Cleavage of the peptide from the resin was performed with 10 cm^3 of TFA, triisopropylosilane, water, and phenol (88:2:5:5) for 2 h at room temperature. The resin was removed by filtration and washed 3 times with TFA (each with 10 cm^3 of TFA). After evaporation of the solvent in vacuo, the resulting oily residue was washed with diethyl ether (3 times) and then lyophilized. Purification was carried out on a Kromasil-5-C8 preparative HPLC column (20 mm × 250 mm) using a linear gradient of 3−8% of an aqueous solution of acetonitrile/0.1% TFA with a flow rate of 15 cm^3/min. The yield was 46.8% (fast atom bombardment mass spectrometry (FAB-MS), $[M + H]^+ = 985.5$; the calculated mass of an observed singly protonated XAO is 985.2 g/mol). The purity of the peptide was also checked by HPLC chromatography, which exhibited a single peak.

2.1.3. Potentiometric Titration. All measurements were carried out at (298.1 ± 0.1) K in an electromotive force (EMF) cell containing a glass electrode and a calomel electrode. The potentiometric microtitration unit was equipped with a computer-aided microtitrator system and a millivoltmeter with an accuracy of 0.01 mV. An ESH 10−00 (Metron) glass microelectrode was used as the indicator electrode, and a calomel EK 10−00 microelectrode was used as the reference electrode. The titrant was added dropwise using a 2.5 cm^3 Hamilton syringe with an accuracy of 0.01 cm^3. For each titration, a stock solution of peptide was prepared at a concentration of approximately 0.001 M; 3 cm^3 of this solution was added to the titration vessel. The solution of the peptide in water was titrated with 0.02 M potassium hydroxide in water, while the solution of the peptide in methanol and dimethyl sulfoxide was titrated with 0.02 M

tetrabutylammonium hydroxide in the appropriate solvent. Because of low concentrations of ionic species, we consider the solutions as ideal solutions.

Before each series of measurements was run, the electrode was calibrated as described below. The pH is related to the electromotive force (E) through the Nernst relationship (eq 1)

$$E = E^\circ - S\,\mathrm{pH} \tag{1}$$

where E° and S are the intercept and the slope, respectively, of the E vs pH curve.

For water, the EMFs of six standard buffer solutions from Merck with pH = 2, 4, 7, 9, 10, and 12, respectively, were measured, and eq 1 was fitted to the measured data. A linear fit was obtained with $E^\circ = 396.0 \pm 5.3$ mV, $S = 57.40 \pm 0.69$ mV.

For methanol and DMSO, the electrode was calibrated against a 2,6-dinitrophenol/tetra-*n*-butylammonium 2,6-dinitrophenolate system with pK_a^{MeOH} (2,6-NO_2PhOH) = 7.8 (ref 32) and pK_a^{DMSO} (2,6-NO_2PhOH) = 4.9 (ref 33). Because 2,6-dinitrophenol is a weak acid, given the total concentration of 2,6-dinitrophenol (C_{HA}) and of its salt (C_{A^-}), the pH can be expressed by eq 2

$$\mathrm{pH} = pK_a - \log\frac{C_{HA}}{C_{A^-}} \tag{2}$$

which results in a linear relationship between E and pH, as expressed by eq 3

$$E = E^\circ - S\,pK_a + S\log\frac{C_{HA}}{C_{A^-}} \tag{3}$$

Linearity of the plot of E vs $\log(C_{HA}/C_{A^-})$ in both MeOH and DMSO was obtained over the range of $\log(C_{HA}/C_{A^-})$ from -1 through 1. To determine E° and S of eq 3 from the intercept and slope of this plot, using the literature values of pK_a, 3 cm^3 of a 0.001 M solution of tetra-*n*-butylammonium 2,6-dichlorophenolate in methanol or DMSO was placed in a thermostated cell and titrated with 0.01 M 2,6-dinitrophenol in the appriopriate solvent (methanol or DMSO, respectively). To maintain constant ionic strength (0.001 M) throughout a titration, a salt solution was added to the titrant in the same concentration as in the titrated solution. We obtained $E^\circ = 583.7 \pm 12.5$ mV and $S = 62.25 \pm 1.48$ mV for methanol and $E^\circ = 366.5 \pm 3.8$ mV and $S = 59.04 \pm 0.63$ mV for DMSO.

2.2. Theoretical Considerations. *2.2.1. Fitting Models of Chemical Equilibria to Titration Curves.* Models of acid−base equilibria were fitted to the resulting titration curves by using the program STOICHIO,[34,35] which is based on a nonlinear confluence analysis. This program can treat any model of chemical equilibria and takes into account all possible sources of experimental error (the error in EMF, titrant and titrated solution volume, reagent impurities, etc.; see refs 34 and 35 for details of the determination of the pK_a values). On the basis of the accuracy of the measurements, we adopted a standard deviation of $\sigma = 2$ mV for XAO in water, methanol, and DMSO (this being the average deviation of the experimental points from the electrode-calibration line). The standard deviation of the titrant volume was assumed to be $\sigma_V = 0.001$ cm^3. Peptide XAO was treated as a tetrafunctional acid, and all four pK_a values were considered as parameters to be determined. The concentration of water in methanol and in DMSO was assumed to be 10^{-2} M with a standard deviation 10^{-2} M.

2.2.2. Theoretical Calculations. As stated in the Introduction, we used two approaches, EDMC/PB/pH and MD/GB/pH, for our calculations. The EDMC/PB/pH method consists of two stages: (i) conformational search with the EDMC method[9,36] with the ECEPP/3[37] + SRFOPT[38] force field and (ii) reevaluation of the energy of the computed conformations using a more accurate energy function, $E(\mathbf{r}_p, \mathrm{pH})$, at conformation, $\mathbf{r}_p$, of the molecule at a given pH, defined by eq 4

$$E(\mathbf{r}, \mathrm{pH}) = E_{int}(\mathbf{r}_p) + F_{cav}(\mathbf{r}_p) + F_{solv}(\mathbf{r}_p) + F_{inz}(\mathbf{r}_p, \mathrm{pH}) \tag{4}$$

where E_{int} ($\mathbf{r}_p$) is the internal conformational energy of the molecule in the absence of solvent, assumed to correspond to the ECEPP/3 energy of the neutral molecule; F_{cav} ($\mathbf{r}_p$) is the free energy associated with the process of cavity creation when transporting the molecule from the gas phase into the solvent; $F_{solv}(\mathbf{r}_p)$ is the free energy associated with the polarization of the solvent; $F_{inz}(\mathbf{r}_p, \mathrm{pH})$ is the free energy associated with the change in the state of ionization of the ionizable groups due to the transfer of the molecule from the gas phase to the solvent, at a fixed pH value.

The polarization free energy is calculated by using the dielectric continuum model to obtain the solution of the Poisson−Boltzmann (PB) equation for the potential of the reaction field with the MBE.[14−16] We used the PARSE[39] atomic charges and radii to evaluate the part of the electrostatic potential coming from the molecule; these charges and radii were tuned to reproduce the electrostatic solvation energies of peptides and proteins in water. A conformational search with the complete energy function defined by eq 4 is prohibitively expensive and lengthy, even taking advantage of parallel processing, because of the necessity to solve the boundary-value problem for the PB equation for each conformation[13−15] to compute the F_{solv} energy component. We, therefore, carry out the conformational search using the EDMC[9,36] method with the ECEPP/3 energy function supplemented with the SRFOPT solvation model and reevaluate the energies of the conformations thus found by using eq 4.[9] The conformational search was carried out assuming that the ornithine and diaminobutyric acid residues were neutral. All EDMC calculations were carried out with the ECEPPAK package.[40,41] A total of about 1000 energy-minimized and accepted conformations were collected, and their energies were reevaluated using eq 4. The EDMC calculations were started from randomly generated structures.

The MD/GB/pH method is based on the GB solvation model, with periodic Monte Carlo sampling of the protonation states. Between Monte Carlo steps, the system evolves according to Newton's equations of motion with the solvation energy computed by using the generalized Born model and a fixed protonation state. At each Monte Carlo step, a titratable site and a new protonation state for that site are chosen randomly. A change in free energy, ΔG, for the protonation or deprotonation (related to the measured EMF values) is calculated according to eq 5[21]

$$\Delta G = k_B T(\mathrm{pH} - pK_{a,ref})\ln 10 + \Delta G_{elec} - \Delta G_{elec,ref} \tag{5}$$

where k_B is the Boltzmann constant, T is the temperature, pH is the specified solvent pH, $pK_{a,ref.}$ is the pK_a of the appropriate reference compound, ΔG_{elec} is the electrostatic component of the change in free energy calculated for the titratable group in the protein, and $\Delta G_{elec,ref}$ is the electrostatic component of the change in free energy for the reference compound. The total change in free energy, ΔG, appears in the Metropolis criterion to determine whether the new charge state will be accepted. If

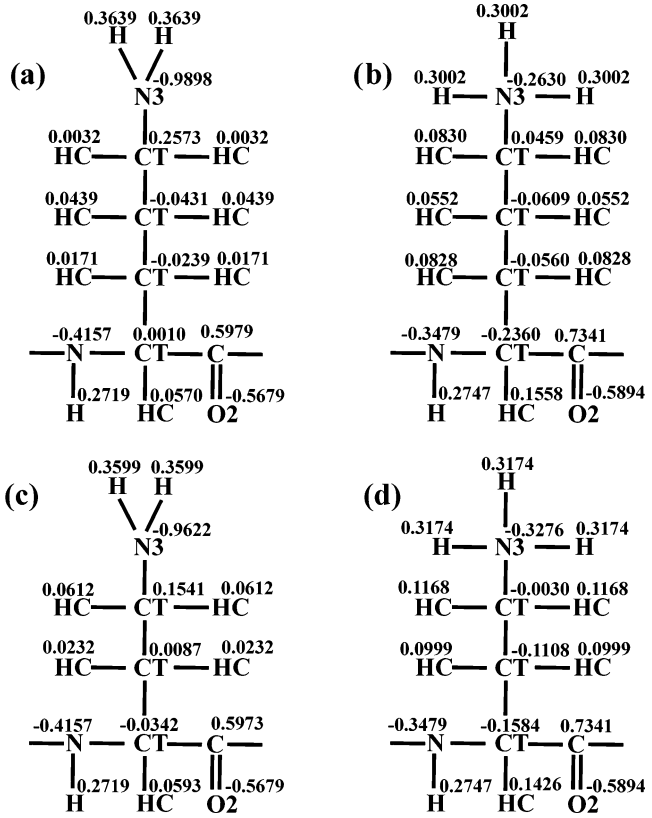

Figure 1. Partial atomic charges (in electron charge units) of the (a) neutral and (b) protonated ornithine residue and the (c) neutral and (d) protonated diaminobutyric acid residue estimated by using the RESP method[42] based on HF/6-31G* calculations carried out with Gaussian 98,[43] used in the calculations with the AMBER force field. The terminal-blocking groups introduced to construct the corresponding model compounds for quantum mechanical calculations are not shown. The atoms are labeled with standard AMBER atom-type symbols.

the new charge state is accepted, MD is continued with the titratable group in the new protonation state; if not, MD continues with no change in the protonation state.

Molecular dynamics calculations were carried out using AMBER 8[20] with the ff99 force field in the NTV ensemble at temperature $T = 300$ K. The integration step was 1 fs. The simulations were run at pH from 2, 3, ..., 14 for water, 4, 5, ..., 15 for methanol, and 4, 5, ..., 18 for DMSO. The range of pH was chosen based on the value of the ionic product of each solvent. One million steps were run for each pH value, and snapshots were collected every 250 steps (a total of 4000 snapshots for every pH value). For computation of the electrostatic solvation energy with the GBSA model, the ionic strength was assumed to be 0.1 M.

The charges of the nonstandard residues, ornithine and diaminobutyric acid, were calculated using the Restricted Electrostatic Potential fit (RESP) method[42] based on HF/6-31G* calculations carried out with Gaussian 98.[43] Ac-O-NHMe and Ac-X-NHMe were used in these calculations to model the ornithine and diaminobutyric acid residues, respectively. The calculated partial charges are shown in Figure 1. (It should be noted that the terminal-blocking groups introduced for the quantum mechanical calculations are not shown in that figure.) Partial charges for other residues were taken from the AMBER 99 database.

To evaluate the F_{cav} and F_{solv} components in eq 4 and to estimate ΔG_{elec} in eq 5, the surface tension and the dielectric constant of the solvent are required. These constants are summarized in Table 1.[31,44−47] As reference compounds, we used

TABLE 1: Physicochemical Constants of Solvents at 298K Used in the Alculations

solvent	abbreviation	σ^a (dyn/cm)	ϵ^b
water	H_2O	72.0[c]	80.0[f]
dimethyl sulfoxide	DMSO	43.5[d]	46.7[f]
95% methanol/5% water		22.6[e]	33.0[g]
methanol	MeOH	22.6[e]	32.6[f]

[a] Surface tension. [b] Dielectric constant. [c] Reference 46. [d] Reference 44. [e] Reference 47; the surface tension of the 95% methanol/5% water mixture was assumed to be the same as for methanol. [f] Reference 45. [g] Reference 31.

n-butylamine (*n*-BuNH_2) for lysine, ethylamine for diaminobutyric acid, and propylamine for the ornithine side chain, respectively. Their pK_a values in water, methanol, 95% methanol/5% water mixture, and DMSO are listed in Table 2.[31,45,48,49]

In the MD/GB/pH approach, canonical sampling of both conformation and protonation state was carried out. Therefore, the average number of protons attached to the peptide molecule at a given pH is computed as a direct average over conformations. In the EDMC/PB/pH approach, which involves noncanonical sampling, the average number of protons of the peptide under study is calculated by Boltzmann averaging over the energies of the conformations of the ensemble as given by eq 6[29]

$$\langle x(\mathrm{pH})\rangle = \frac{\sum_i \langle x_i(\mathrm{pH})\rangle Z_i}{\sum_i Z_i} \tag{6}$$

where Z_i is the partition function of conformation i defined by eq 7

$$Z_i = \sum_{n=1}^{2^N} \exp[-\beta \Delta G(\mathrm{pH}, \xi_i^{(n)}) \tag{7}$$

where N is the number of ionizable groups and $\Delta G(\mathrm{pH}, \xi_i^{(n)})$ is the Gibbs free energy of the ith conformation in the nth ionization state $\xi^{(n)}$. Each $\langle x_i(\mathrm{pH})\rangle$ is an average over the protonation states of the molecule in a particular conformation, and eq 6 averages these averages over conformational states. The value of β in eq 7 corresponds to $T = 298$ K.

To compare the theoretical titration curves of peptide XAO for both approaches (EDMC/PB/pH and MD/GB/pH) with the corresponding experimental titration curves, we converted, $\langle x(\mathrm{pH})\rangle$ into volume of added titrant (V(pH)) as given by eq 8

$$V(\mathrm{pH}) = \frac{\{\langle 4 - x(\mathrm{pH})\rangle C_p - 10^{-\mathrm{pH}} + C_w 10^{(\mathrm{pH}-\mathrm{p}K_{aw})}\}}{C_{OH} + 10^{-\mathrm{pH}} - C_w 10^{(\mathrm{pH}-\mathrm{p}K_{aw})}} V_p \tag{8}$$

where C_p is the concentration of the peptide in the titrated solution, V_p is the volume of the titrated solution, C_{OH} is the concentration of the titrant, C_w is the concentration of water in the solution for nonaqueous solvents, and K_{aw} is the acid-dissociation constant of water in the given solvent. For nonaqueous solvents, traces of water must be taken into account because traces of water on the order of 10^{-3} M can act as a base or an acid even comparable to the concentration of reagents in potentiometric titrations.[50]

For Ac-K_5-NHMe, we used $\langle x(\mathrm{pH})\rangle$ directly without conversion to V(pH).

3. Results and Discussion

Figure 2 presents the theoretically calculated and experimental[31] pH titration curves for Ac-K_5-NHMe peptide in the 95%

TABLE 2: pK_a Values of Reference Model Compounds at 298 K Used in the Calculations

model	amino acid	pK_a in H_2O	pK_a in MeOH	pK_a in DMSO	pK_a in 95% methanol/5% water
n-buthylamine	lysine			9.7[a]	10.0[b]
ethylamine	diaminobutyric acid	10.87[c]	11.0[d]	11.0[d]	
propylamine	ornithine	10.71[c]	12.65[e]	10.4[e]	

[a] Reference 48. [b] Taken as the pH corresponding to the protonation of 50% *n*-$BuNH_3^+$ from Figure 2 in ref 31 [c] Reference 49. [d] Reference 45. [e] Results in this work from potentiometric titration.

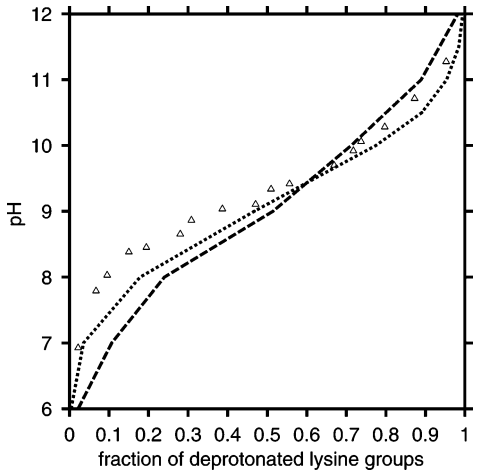

Figure 2. Comparison of the experimentally determined titration curve of polylysine (triangles; ref 31) with the curve calculated by using the EDMC/PB/pH method (dashed line; ref 29) and the MD/GB/pH method (dotted line; this work).

MeOH/5% water mixture. It can be seen that there is qualitatively good agreement between the theoretical titration curves and the experimental data. The calculated pK_a corresponding to the pH at the 0.5 ionization degree agrees well with the experimental value. However, the experimental titration points form a steeper curve for lower pH values than the curve[29] calculated by using the EDMC/PB/pH procedure or the curve calculated by using the MD/GB/pH procedure. This means that both the EDMC/PB/pH and MD/GB/pH methods predict more stepwise deprotonation (i.e., the molecule behaves as a weak multifunctional acid with small but noticeable differences between the consecutive acidity constants) of this sequence than found experimentally, suggesting that the screening effect of the solvent is too weak in the theoretical models. However the MD/GB/pH method gives better agreement (i.e., the theoretically calculated experimental curves is closer to the experimental points) between experiment and theory.

The experimental potentiometric titration curves of peptide XAO determined in water, methanol, and DMSO are shown in Figure 3. It can be seen that the model of four stepwise dissociation equilibria (subsection 2.2.1) fits the experimental points very well for all three solvents. The first pK_a value is remarkably lower than the remaining three (Table 3), which is manifested as a big jump in the titration curves (Figure 3). In addition, pK_{a3} and pK_{a4} in DMSO differ from each other more than pK_{a2} and pK_{a3}, which is manifested in the titration curve as an additional jump (Figure 3C).

The experimental titration curves are compared with theoretical ones in Figure 4. It can be seen that the curves calculated with the EDMC/PB/pH method in water and methanol exhibit a smooth shape characteristic of titration curves of multifunctional acids with weakly differentiated dissociation costants, in contrast to the experimental curves. The curve calculated in DMSO exhibits a jump corresponding to the release of the fourth

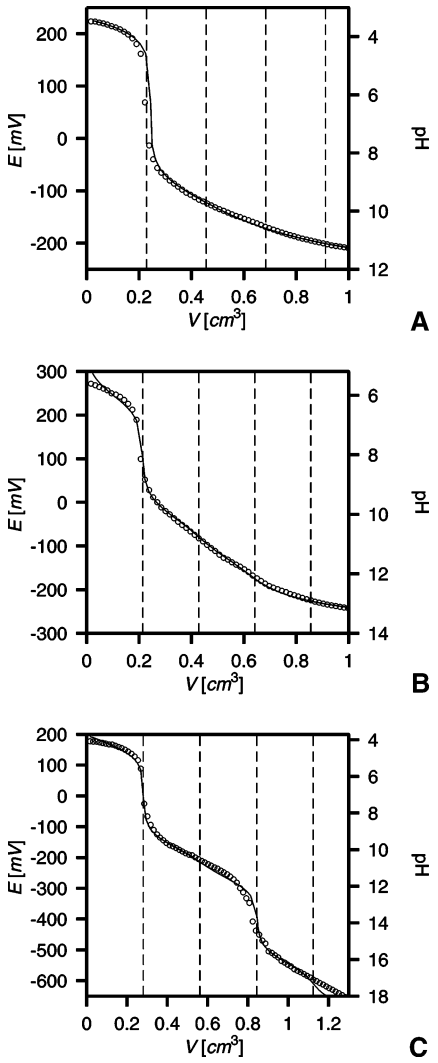

Figure 3. Experimental titration curves of XAO in (A) water, (B) methanol, and (C) DMSO. Experimental points are shown as circles, and the curves corresponding to the best-fitting equilibrium models as solid lines. Dashed vertical lines are drawn at the titrant volumes corresponding to the release of 1, 2, 3, and 4 mol of protons per mol of XAO, respectively.

proton; however, this jump does not occur on the experimentally determined titration curve.

The curves obtained with the MD/GB/pH method are closer to the experimental curves than those obtained with the EDMC/PB/pH approach. The MD/GB/pH curves for methanol and DMSO also have shapes close to those of the corresponding experimental curves with jump regions in similar positions. For these two solvents, the MD/GB/pH approach predicts that the first proton is released easier than the remaining ones, in agreement with the experimental results. However, the first jump is not as large as measured experimentally, demonstrating that theory underestimates the effect of the peptide microenvironment on pK_a. It is remarkable that the worst agreement is observed

TABLE 3: Four pK_a Values of Peptide XAO in Water, Methanol, and DMSO, at 298.1 K, Obtained by Fitting the Equilibrium Model of Dissociation to the Potentiometric Titration Curves

	water	methanol	DMSO
pK_{a1}	2.72 (0.13)[a]	5.44 (0.44)	4.67 (0.13)
pK_{a2}	8.98 (0.04)	9.90 (0.06)	9.62 (0.15)
pK_{a3}	10.17 (0.04)	11.51 (0.06)	10.05 (0.16)
pK_{a4}	11.06 (0.08)	13.37 (0.1)	12.00 (0.16)
pK_{aw}[b]	15.7[c]	13.91 (0.07)	17.61 (0.16)

[a] Numbers in parentheses are the standard deviations. [b] This is the pK of water in the given solvents. [c] In water, pK_{aw} was not an adjustable parameter, and the value of 14 was assumed for the negative of the logarithm of the ionic product of water (pK_w).

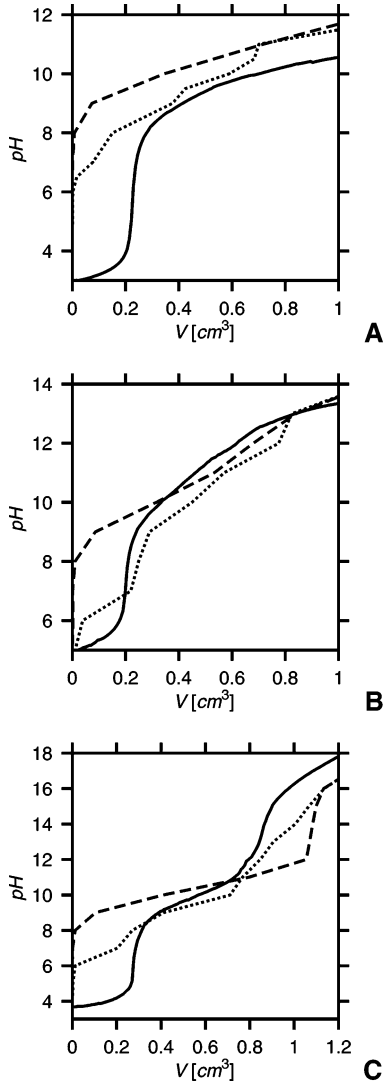

Figure 4. Comparison of experimentally determined (solid lines) and calculated titration curves of XAO by using the EDMC/PB/pH (dashed lines) and MD/GB/pH (dotted lines) in (A) water, (B) methanol, and (C) DMSO. Discontinuities in the calculated curves arise because of sampling only at integral values of pH.

for water; for this solvent, the MD/GB/pH method fails to predict even the qualitative shape of the experimental titration curve. It is likely that the poorer performance of this method for water than for the nonaqueous solvents is caused by a greater role of specific solvation in water than in the two nonaqueous solvents considered here.

As mentioned in the Introduction, the advantage of the MD/GB/pH over the EDMC/PB/pH method is that the same energy

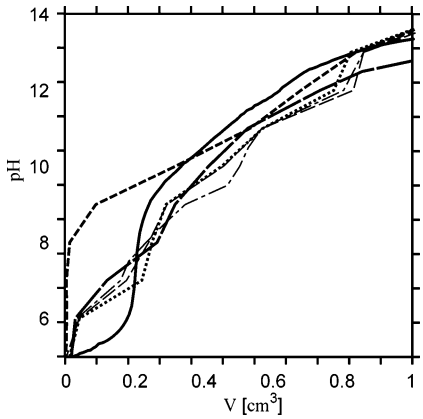

Figure 5. Comparison of the experimental titration curve of XAO in methanol (solid line) with the curve calculated with the EDMC/PB/pH approach (heavy, short-dashed lines); the curves calculated with the MD/GB/pH approach for different starting conformations (random (as in Figure 4B; dotted lines), extended (thin-dashed lines), and α-helical (dot−dashed lines)); and the curve calculated with the MD/GB/pH approach where the conformations were generated in an MD run with all basic groups charged and subsequently subjected to sampling protonation states without changing conformation (heavy, long-dashed lines).

function is implemented in conformational sampling and in sampling protonation states at different pH values. This could be the reason that better agreement with the experimental data was obtained for the titration curves calculated with the MD/GB/pH approach than with those calculated with the EDMC/PB/pH approach. However, the two approaches use different potential energy functions and different solvation models, and consequently, the AMBER force field with the GB solvation model might describe the conformational free energy surface with variable protonation state better than the ECEPP/3 force field with the PB-based solvation model does.

To determine the primary reason for the better performance of the MD/GB/pH approach, we carried out additional calculations with the AMBER force field and GB model for XAO in methanol (for this system, the difference in the performance of the two approaches is particularly striking; see Figure 4B). First, we carried out an MD run with all diaminobutyric acid and ornithine residues charged. The resulting conformations were subsequently clustered into families, and the leading members of 200 families with the lowest potential energies were selected. Each of these 200 conformations was subjected to short (25 000 steps) constant-pH MD runs at all pH values considered with a very small time step $\delta t = 0.01$ fs and sampling the protonation states at each time step. With such a treatment, a conformation practically does not change; therefore it effectively corresponds to the procedure of sampling the protonation states of fixed conformations from the EDMC/PB/pH approach. In addition to this, we carried out two regular MD/GB/pH runs starting from the extended and the α-helical conformation of XAO, respectively. The computed titration curves are shown in Figure 5, together with the experimental curve and the curve computed with the EDMC/PB/pH approach. It can be seen that the agreement of the curve computed with the modified MD/GB/pH approach (sampling of protonation states of *fixed* conformations; long-dashed line in Figure 5) to the experimental curve is qualitatively similar to those of the curves computed with the full-blown MD/GB/pH approach (dotted line, thin-dashed line, and dot−dashed lines in Figure 5), and the agreement is much better than for the curve calculated with the EDMC/PB/pH approach (heavy, short-dashed line in Figure 5). Thus, the better performance of the MD/GB/pH approach over the EDMC/

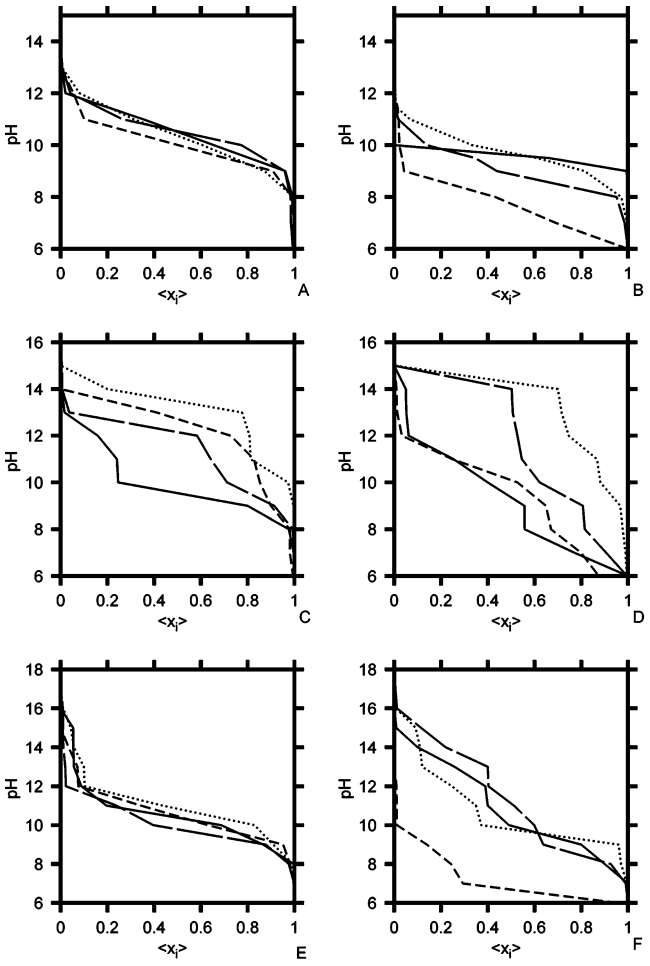

Figure 6. Plots of the computed pH vs the degree of protonation ($\langle x_i \rangle$) of the four titratable groups of XAO obtained by using the EDMC/PB/pH method in (A) water, (C) methanol, and (E) DMSO, and the MD/GB/pH method in (B) water, (D) methanol, and (F) DMSO. Solid line, X2; dashed line, X3; dotted line, O11; long-dashed line, O12 (the number following the one-letter symbol of an amino acid residue indicates its position in the sequence). See text for the explanation of one-letter symbols of residues. Discontinuities in the calculated curves arise because of sampling only at integral values of pH (long-dashed lines).

PB/pH approach seems to be caused by the differences in the force fields and solvation models rather than by the differences in the sampling schemes. It should be noted, however, that the difference between the curve computed with the modified MD/GB/pH approach and the curves computed with the full-blown approach is greater at higher pH values than the differences between the curves computed with the full-blown MD/GB/pH starting from different conformations; this reflects the change of conformational ensemble with pH.

The pH is plotted as a function of the degree of protonation of the titratable groups, $\langle x_i \rangle$, in Figures 6A−F. It can be seen that the EDMC/PB/pH approach predicts that all groups deprotonate to a comparable extent in water and DMSO, while there is some differentiation in the degree of protonation in methanol at medium pH (Figure 6C). This differentiation is, however, not sufficient to produce a jump in the predicted titration curve (Figure 4B), and the EDMC/PB/pH method predicts that XAO behaves as a weak multifunctional acid in methanol with small differences between consecutive pK_a values. Conversely, the MD/GB/pH method predicts that the protonation states are more differentiated even in water, for which the theoretically calculated titration curve is in poor agreement with the experimental curve. On the basis of the results of MD/GB/pH calculations, it can be concluded (Figures 6B, 6D, and 6F) that X2 or X3 (where the number after the one-letter symbol of the amino acid residue denotes its position in the sequence) is the first to deprotonate. However, it can be seen that, except for the first jump in the calculated titration curve in DMSO (Figure 4C) where X3 is clearly the first to deprotonate (Figure 6F), and consequently, based on the results of the MD/GB/pH calculations, pK_{a1} can be assigned to X3, the jumps in the theoretically calculated titration curves do not correspond to complete deprotonation of a given group, but rather to partial deprotonation of a few groups. Therefore, in the case of flexible peptides, a "pK_a value" does not seem to have the meaning of a constant characteristic of a given functional group but should be considered as an average over those functional groups that contribute to the release of the next proton within a given pH range. This is understandable, because flexible peptides form ensembles of interconverting conformations.

An analysis of the conformations of XAO obtained in the EDMC and constant-pH MD runs (not shown here) reveals that the calculated conformations of XAO are variations of an α-helix melted or broken in several places, independent of pH. This result does not agree with the suggestion from experimental data that the peptide occurs in polyproline II and extended conformations.[30] This discrepancy suggests that the AMBER force field might be biased toward α-helical structure even if the coupling between pH and conformation is taken into account. Because the purpose of this study was to assess the ability of theoretical methods to reproduce potentiometric titration curves of XAO, we leave the detailed analysis of the conformational ensembles (including a comparison of the theoretically calculated observables with those determined from circular dichroism and NMR spectra) to a further paper (Makowska et al., paper in preparation).

Conclusions

We compared the potentiometric titration curves of Ac-K_5-NHMe and Ac-XX(A)$_7$OO-NH_2 (XAO) calculated by using two theoretical methods, EDMC/PB/pH and MD/GB/pH, respectively, of pH-dependent conformational analysis with the experimental curves reported in the literature[31] and determined in this work, respectively. Both methods give qualitatively comparable predictions for Ac-K_5-NHMe where differentiation of proton affinity of the ionizable groups is weak, the MD/GB/pH method, however, providing better quantitative agreement. For XAO, for which the proton affinity is clearly differentiated, resulting in clear jumps in the titration curves, the MD/GB/pH method is clearly superior to EDMC/PB/pH because it predicts correct titration profiles in methanol and DMSO qualitatively, while the EDMC/PB/pH method fails to do so. The reason for this seems to be the difference in the force fields and solvation models and not in sampling schemes. It should be noted, though, that even the MD/GB/pH approach does not provide quantitative agreement with experiment. Remarkably, the agreement between theory and experiment is poorer for water than for nonaqueous solvents (methanol and DMSO), which suggests a greater role for specific solvation in water.

Acknowledgment. This work was supported by grants from the Polish Ministry of Education and Science (1 T09A 101 30), the U. S. National Institutes of Health (GM-14312), and the U. S. National Science Foundation (MCB00-03722), This research was conducted by using the resources of (a) our 676-processor Beowulf cluster at the Baker Laboratory of Chemistry and

Chemical Biology, Cornell University, (b) the National Science Foundation Terascale Computing System at the Pittsburgh Supercomputer Center, (c) our 45-processor Beowulf cluster at the Faculty of Chemistry, University of Gdańsk, (d) the Informatics Center of the Metropolitan Academic Network in Gdansk, and (e) the Interdisciplinary Center of Mathematical and Computer Modeling at the University of Warsaw.

References and Notes

(1) Linderstrøm-Lang, K. *Compt. Rend. Trav. Lab. Carlsberg, Ser. Chim.* **1924**, *15*, 29.
(2) Laskowski, M., Jr.; Scheraga, H. A. *J. Am. Chem. Soc.* **1954**, *76*, 6305.
(3) Gilson, M. K.; Honig, B. H. *Proteins: Struct., Funct., Genet.* **1988**, *3*, 32.
(4) Demchuk, E.; Wade, R. C. *J. Phys. Chem.* **1996**, *100*, 17373.
(5) Wlodek, S. T.; Antosiewicz, J.; McCommon, J. A. *Protein Sci* **1997**, *6*, 373.
(6) Nielsen, J. E.; Vriend, G. *Proteins*: *Struct., Funct., Genet.* **2001**, *43*, 403.
(7) Vorobjev, Y. N.; Scheraga, H. A.; Hitz, B.; Honig, B. *J. Phys. Chem.* **1994**, *98*, 10940.
(8) Vorobjev, Y. N.; Scheraga, H. A.; Honig, B. *J. Phys. Chem.* **1995**, *99*, 7180.
(9) Ripoll, D. R.; Vorobjev, Y. N.; Liwo, A.; Vila, J. A.; Scheraga, H. A. *J. Mol. Biol.* **1996**, *264*, 770.
(10) Ripoll, D. R.; Liwo, A.; Scheraga, H. A. *Biopolymers* **1998**, *46*, 117.
(11) Vila, J. A.; Ripoll, D. R.; Villegas, M. E.; Vorobjev, Y. N.; Scheraga, H. A. *Biophys. J.* **1998**, *75*, 2637.
(12) Vila, J. A.; Ripoll, D. R.; Vorobjev, Y. N.; Scheraga, H. A. *J. Phys. Chem. B* **1998**, *102*, 3065.
(13) Vila, J. A.; Ripoll, D. R.; Arnautova, Y. A.; Vorobjev, Y. N.; Scheraga, H. A. *Proteins: Struct., Funct., Bioinf.* **2005**, *61*, 56.
(14) Vorobjev, Y. N.; Grant, J. A.; Scheraga, H. A. *J. Am. Chem. Soc.* **1992**, *114*, 3189.
(15) Vorobjev, Y. N.; Scheraga, H. A. *J. Phys. Chem.* **1993**, *97*, 4855.
(16) Vorobjev, Y. N.; Scheraga, H. A. *J. Comput. Chem.* **1997**, *18*, 569.
(17) Baptista, A. M.; Teixeira, V. H.; Soares, C. M. *J. Chem. Phys.* **2002**, *117*, 4184.
(18) Walczak, A. M.; Antosiewicz, J. M. *Phys. Rev. E* **2002**, *66*, 051911.
(19) Bürgi, R.; Kollman, P. A.; Gunsteren, W. F. *Proteins: Struct., Funct., Genet.* **2002**, *47*, 469.
(20) Case, D. A.; Darden, T. A.; Cheatham, T. E., III.; Simmerling, C. L.; Wang, J.; Duke, R. E.; Luo, R.; Merz, K. M.; Pearlman, D. A.; Crowley, M.; Brozell, S.; Tsui, V.; Gohlke, H.; Mongan, J.; Hornak, V.; Cui, G.; Beroza, P.; Schafmeister, C.; Caldwell, J. W.; Ross, W. S.; Kollman, P. A. *AMBER 8*; University of California: San Francisco, 2004.
(21) Mongan, J.; Case, D. A.; McCammon, J. A. *J. Comput. Chem.* **2004**, *25*, 2038.
(22) Gilson, M. K.; Honig, B. H. *Nature* **1987**, *330*, 84.
(23) Soman, K.; Yang, A. S.; Honig, B.; Fletterick, R. *Biochemistry* **1989**, *28*, 9918.
(24) Sharp, K. A. *Proteins: Struct., Funct., Bioinf.* **1998**, *33*, 39.
(25) Börjesson, U.; Hünenberger, P. H. *J. Phys. Chem. B* **2004**, *108*, 13551.
(26) Dlugosz, M.; Antosiewicz, J. M.; Robertson, A. *Phys. Rev. E* **2004**, *69*, 021915.
(27) Kuhn, B.; Kollman, P. A.; Stahl, M. *J. Comput. Chem.* **2004**, *25*, 1865.
(28) Mongan, J.; Case, D. *Curr. Opin. Struct. Biol.* **2005**, *15*, 157.
(29) Makowska, J.; Baginska, K.; Kasprzykowski, F.; Vila, J. A.; Jagielska, A.; Liwo, A.; Chmurzynski, L.; Scheraga, H. A. *Biopolymers* **2005**, *80*, 214.
(30) Shi, Z.; Olson, C. A.; Rose, G. D.; Baldwin, R. L.; Kallenbach, N. R. *Proc. Natl. Acad. Sci. U.S.A.* **2002**, *99*, 9190.
(31) Liem, R. K. A.; Poland, D.; Scheraga, H. A. *J. Am. Chem. Soc.* **1970**, *92*, 5717.
(32) Chmurzynski, L.; Pawlak,Z. *J. Chem. Thermodyn.* **1998**, *30*, 27.
(33) Kolthoff, I. M.; Chantooni, M. K.; Bhowmik, S. *J. Am. Chem. Soc.* **1968**, *90*, 23.
(34) Kostrowicki, J.; Liwo, A. *Comput. Chem.* **1987**, *11*, 195.
(35) Kostrowicki, J.; Liwo, A. *Talanta* **1990**, *37*, 645.
(36) Ripoll, D. R.; Scheraga, H. A. *Biopolymers* **1988**, *27*, 1283.
(37) Nemethy, G.; Gibson, D.; Palmer, K. A.; Yoon, C. N.; Paterlini, G.; Zagari, A.; Rumsey, S.; Scheraga, H. A. *J. Phys. Chem.* **1992**, *96*, 6472.
(38) Vila, J. A.; Williams, R. L.; Vasquez, R. L.; Scheraga, H. A. *Proteins: Struct., Funct., Genet.* **1991**, *10*, 199.
(39) Sitkoff, D.; Sharp, K. A.; Honig, B. *J. Phys. Chem.* **1994**, *98*, 1978.
(40) Ripoll, D. R.; Pottle, M. S.; Gibson, K. D.; Liwo, A.; Scheraga, H. A. *J. Comput. Chem.* **1995**, *16*, 1153.
(41) Ripoll, D. R.; Liwo, A.; Czaplewski, C. *TASK Q.* **2000**, *3*, 313.
(42) Bayly, C. I.; Cieplak, P.; Cornell, W. D.; Kollman, P. A. *J. Phys. Chem. A* **1993**, *97*, 10269.
(43) Frisch, M. J.; Trucks, G. W.; Schlegel, H. B.; Scuseria, G. E.; Robb, M. A.; Cheeseman, J. R.; Zakrzewski, V. G.; Montgomery, J. A., Jr.; Stratmann, R. E.; Burant, J. C.; Dapprich, S.; Millam, J. M.; Daniels, A. D.; Kudin, K. N.; Strain, M. C.; Farkas, O.; Tomasi, J.; Barone, V.; Cossi, M.; Cammi, R.; Mennucci, B.; Pomelli, C.; Adamo, C.; Clifford, S.; Ochterski, J.; Petersson, G. A.; Ayala, P. Y.; Cui, Q.; Morokuma, K.; Malick, D. K.; Rabuck, A. D.; Raghavachari, K.; Foresman, J. B.; Cioslowski, J.; Ortiz, J. V.; Stefanov, B. B.; Liu, G.; Liashenko, A.; Piskorz, P.; Komaromi, I.; Gomperts, R.; Martin, R. L.; Fox, D. J.; Keith, T.; Al-Laham, M. A.; Peng, C. Y.; Nanayakkara, A.; Gonzalez, C.; Challacombe, M.; Gill, P. M. W.; Johnson, B. G.; Chen, W.; Wong, M. W.; Andres, J. L.; Head-Gordon, M.; Replogle, E. S.; Pople, J. A. *Gaussian 98*, revision A.11.4; Gaussian, Inc.: Pittsburgh, PA, 1998.
(44) Clever, L. H.; Snead, C. C. *J. Phys. Chem.* **1963**, *67*, 918
(45) Bos, M.; van der Linden, W. E. *Anal. Chim. Acta* **1996**, *332*, 201.
(46) Compostizo, A.; Cancho, S. M.; Rubio, R. G.; Colin, A. C. *Phys. Chem. Chem. Phys.* **2001**, *3*, 1861.
(47) Wu, M. M.; Cubaud, T.; Ho, C. M. *Phys. Fluids* **2004**, *16*, L51.
(48) Zielinska, J.; Makowski, M.; Maj, K.; Liwo, A.; Chmurzynski, L. *Anal. Chim. Acta* **1999**, *401*, 317.
(49) Tehan, B. G. *Quant. Struct−Act. Relat.* **2002**, *21*, 473.
(50) Liwo, A.; Sokolowski, K.; Wawrzynów, A.; Chmurzynski, L. *J. Solution Chem.* **1990**, *19*, 1113.